Effect of Molecular and Lattice Structure on Hydrogen Transfer in Molecular Crystals of Diamino-dinitroethylene and Triamino-trinitrobenzene

Anna V. Kimmel

Department of Physics, University of Nevada, Las Vegas, Nevada 89154

Peter V. Sushko and Alexander L. Shluger

London Centre for Nanotechnology and Department of Physics and Astronomy, Materials Simulation Laboratory, University College London, Gower Street, London WC1E 6BT, UK

Maija M. Kuklja*

Department of Materials Science and Engineering, University of Maryland, College Park, Maryland 20742

Received: January 31, 2008; Revised Manuscript Received: February 28, 2008

We have studied the intra- and intermolecular hydrogen transfer in a crystalline 1,1-diamino-2,2-dinitroethylene (DADNE) and 1,3,5-triamino-2,4,6-trinitrobenzene (TATB) by means of an embedded cluster method and density functional theory (DFT). We found that, even though both of these materials have similar amino- and nitro- functional groups and layered crystalline structures, there are important differences in the mechanisms of hydrogen transfer. In particular, our calculations suggest that the proton migration from an amino-group to a nitro-group of the *same* molecule is a feasible process in TATB but not in DADNE. At the same time, we have found that no *intermolecular* hydrogen transfer occurs in either molecular crystal. These results imply that the activation of the decomposition reactions proceeds via different paths in these two materials.

Introduction

The mechanisms of processes underlining high performance and low sensitivity of energetic materials are the subject of ongoing debate.[1,2] In particular, 1,1-diamino-2,2-dinitroethylene (DADNE)[3,4] has recently attracted substantial interest because it is expected that its sensitivity can be as low as that of well-studied 1,3,5-triamino-2,4,6-trinitrobenzene (TATB)[5,7] since both materials have the same set of molecular functional groups (see Figures 2a and 3a). In this work, we argue that the efficiency of hydrogen-mediated processes, which are thought to be responsible for the unprecedented stability of TATB,[5,7] is determined not only by the presence of characteristic functional groups but also by the structure of the molecular backbone, molecular polarity, and the structure of the crystalline lattice. Our *ab initio* embedded cluster calculations highlight differences in hydrogen migration processes in TATB and DADNE. Consequently, the initiation of chemical decomposition in these materials proceeds via different pathways.

Among the initiation pathways for the decomposition of nitro-explosives, such as DADNE and TATB, those involving C-NO_2 bond fission as well as formation of CONO and/or HONO isomers are thought to be the most feasible.[1,2,5,8–11] The HONO isomer in TATB, for example, can be formed via an intramolecular hydrogen transfer from an amino- to a nitro- group.[8] In particular, previous molecular calculations[8] suggested that HONO isomers serve as precursors for the formation of benzofurazan and benzofuraxan derivatives, which are relatively insensitive to external stimuli.[5,7] This model is consistent with experiments in which the TATB decomposition has been stimulated using thermal treatment, electron beam, UV photolysis, mechanical impact, and shock.[5,7] Much less is known, however, about similar processes in DADNE.

Although both TATB and DADNE crystals have layered structures, there are important differences: the nonsymmetric polar DADNE molecules are arranged into zigzag-shaped parallel polar layers (see Figure 1b), while the symmetric nonpolar TATB molecules are organized in nearly flat, graphitelike sheets (Figure 1b). Similarities of TATB and DADNE molecular structures (Figure 1), the absence of a melting point,[2,3] and the presence of water and NO species among the DADNE decomposition products[3,4,12] suggest the existence of hydrogen transfer channels in this material, which potentially can act as a trigger for the overall thermal decomposition,[1] similarly to TATB. In this paper, we use theoretical modeling to explore the effect of differing crystalline structures on the hydrogen transfer, which is defined hereafter as a process of hydrogen migration from an amino- to a neighbor nitro- group accompanied by switching of hydrogen bonds.

Computational Details

To reveal the effect of the crystalline structure on the hydrogen migration in TATB and DADNE, we have studied their electronic and geometric structures by means of an embedded cluster method (ECM) as implemented in GUESS computer code,[13–16] which is linked to Gaussian03 package[17] for quantum-mechanical calculations of molecules. This is a hybrid quantum mechanics/molecular mechanics technique in which a small region, considered quantum mechanically (QM cluster), is embedded into a classically treated environment (Figure 1c). The method takes into account the interaction of the QM cluster with the rest of the host lattice, the perturbation of the lattice by the defect, and the reciprocal effect of the lattice polarization on the defect itself. This is achieved by constructing

* Corresponding author.

10.1021/jp800930d CCC: $40.75
Published on Web 04/16/2008

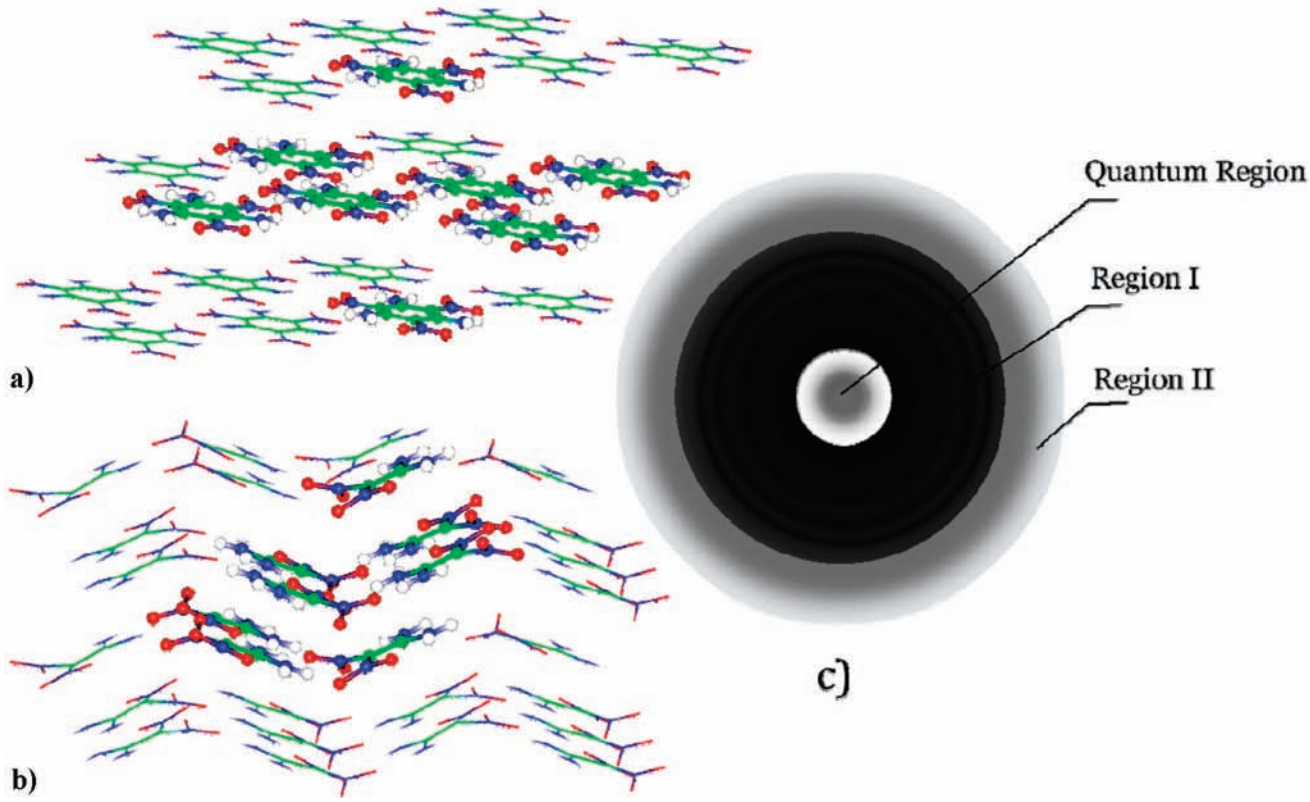

Figure 1. Structures of TATB (a) and DADNE (b) molecular crystals. TATB has planar graphitelike layers. DADNE consists of zigzaglike layers. Eight-molecule quantum mechanical (QM) clusters are shown using the ball and stick model on the background of the respective host lattices, which are shown using the sticks only. (c) Setup used for the embedded cluster calculations. Atoms in region I, including the QM cluster, are fully relaxed, while atoms in region II are fixed.

an external potential, produced by a polarizable lattice, in which the cluster is then embedded. One of the main advantages of this method is that it allows us to take into consideration the full extent of the lattice distortion and ion polarization induced by the defect, e.g., transferred hydrogen.

In our method, each molecular crystal is represented using a spherical nanoscale cluster built out of unit cell "building blocks" so as to enforce a charge neutrality and zero dipole moment of the nanocluster (Figure 1). The nanocluster is divided into an inner spherical region I, where all atoms are relaxed, and an outer region II, where all atoms are fixed in their crystalline lattice sites. The purpose of region II is to mimic the infinite crystalline environment for atoms in region I and to accurately reproduce the Coulomb and short-range interactions with these atoms. Molecular building blocks are assigned either to region I or region II as a whole, so as no intramolecular bonds are broken. The region I is further divided into two subregions: several molecules at its center form a QM cluster, while the rest of the molecules are treated classically. The total energy (see also ref 15) includes contributions from (i) the energy of the QM cluster in the external electrostatic potential due to the remaining part of the system calculated using DFT (for that, the matrix elements of the electrostatic potential are included into the Kohn−Sham equations, which are solved for electrons of the QM cluster), (ii) the intermolecular interaction of the classically treated molecules with each other and with the molecules of the QM cluster, and (iii) intramolecular interactions within the classically treated molecules in the region I. The last two terms are described using a classical force-field. In particular, the intermolecular interactions are represented using both Lennard-Jones and Coulomb potentials, while the intramolecular interactions are represented using Morse potentials as well as three- and four-body potentials. These contributions to the total energy and the details of the parametrization for the molecular crystals are detailed elsewhere.[16] The hydrogen transfer takes place within the QM cluster, and therefore, the corresponding interactions are considered fully quantum-mechanically.

In this work, the TATB and DADNE crystals were modeled using nanoclusters with the radii of about 20 Å, which include 300 and 292 TATB and DADNE molecules, respectively. In the case of DADNE, the radius of the region I was set to 10 Å so that 35 molecules are fully relaxed. The radii of these regions are chosen so as to provide convergence of the electrostatic potential inside region I and to accommodate the lattice distortions induced by the atomic and electronic structure changes that take place in the QM cluster. The TATB molecules are more rigid than DADNE due to their benzene rings. Moreover, the TATB lattice is stabilized by the $\pi-\pi$ stacking. Therefore, local chemical reactions are expected to induce only a short-range lattice relaxation, which can be accounted for by only fully optimizing the geometry of the QM cluster. Therefore the TATB molecules outside the QM cluster were kept fixed.

The electronic structures of TATB and DADNE were calculated using the eight-molecule QM clusters shown in Figure 1a and b. In each case, the QM cluster configuration is chosen from symmetry and topology considerations, so as to provide zero total charge and dipole moment to avoid artificial electrostatic effects. The calculations were carried out using the hybrid B3LYP density functional[18,19] and the 6-21G basis set. It has been established that this basis set provides sufficient variational freedom for the calculations of molecular crystals.[20,21] In addition, we checked that the 6-21G, 6-31G and 6-31+G* basis

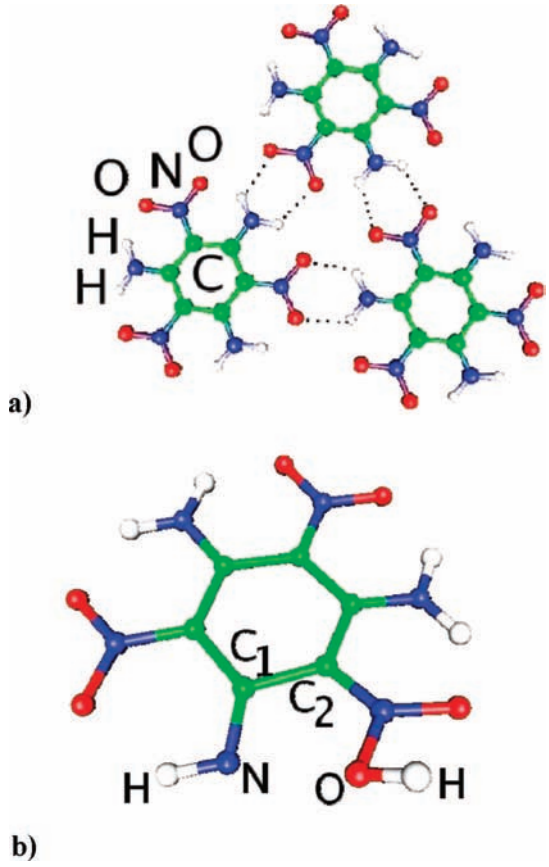

Figure 2. Arrangement of TATB molecules in a crystalline layer. (a) TATB's three equivalent locations of adjacent nitro- and amino- groups, where an intermolecular hydrogen transfer may occur (broken lines). (b) Molecular structure of the TATB molecule after HONO transformation. A torsion angle of donor amino- group $\angle H-N-C_1-C_2$ is equal to 9.4°, and a torsion angle of hydrogen bearing nitro- group $\angle O-O-N-C_2$ is equal to −3.9°.

sets produce the very similar geometry and electronic structure of crystalline DADNE.

Parameters of the intramolecular potentials for DADNE were initially fitted so as to reproduce vibrational frequencies of an isolated molecule obtained using the 6-311+G* basis set and B3LYP density functional[22] and, then, readjusted to obtain a better agreement with the crystalline geometry. The intermolecular potentials obtained for rigid DADNE molecules[23] were optimized in order to reproduce the DADNE crystalline structure. The positions of all atoms inside the region I are optimized using the standard Broyden−Fletcher−Goldfarb−Shanno algorithm. The charge density distribution in both TATB and DADNE has been characterized using the natural population analysis (NPA).[24]

Our ECM calculations yield the equilibrium geometries of the perfect TATB and DADNE crystals in good agreement with the experiment.[4,25] For example, the intramolecular torsion angles (see Figure 3b) $N_1-C-C-N_3$ and $N_1-C-C-N_4$ for DADNE molecules in the QM cluster are equal to −4.7° and −178°, to be compared with their experimental values of −4.7° and −177°, respectively. The intermolecular distances between amino nitrogen and nitro oxygen are 3.03 and 2.69 Å in DADNE (experimental values are 3.0 and 2.61 Å)[4] and 2.97 Å in TATB (experimental value is 2.99 Å).[25] A set of careful tests performed to probe the quality of the developed ECM model convinced us that the technique is appropriate to study chemistry in DADNE and related materials.

Results and Discussion

In previous studies, the hydrogen transfer in crystalline TATB has been modeled using one or two isolated and partially constrained TATB molecules.[8] These calculations, which have been carried out using several density functionals and basis sets, propose that both the intramolecular and intermolecular hydrogen transfers are possible with the reaction energies of 35.0–45.6 and 64.3–72.4 kcal/mol for the intra- and intermolecular transfer, respectively. Our calculations using the same setup, B3LYP functional and 6-31+G** and 6-21G basis sets, give a very similar range of the reaction energies: 36.0 and 47.5 kcal/mol for the intramolecular H transfer and 67.1 and 72.3 kcal/mol for the intermolecular H transfer. However, modeling a TATB crystal using isolated constrained molecules neglects the crystalline potential and does not take into account possible displacements of a molecule as a whole. Consequently, the conclusions obtained using such a model may not apply to the solid phase.[26,27]

Our ECM calculations yield the one-electron band gap of TATB of 3.07 eV. This can be compared with the results of previous periodic Hartree−Fock (HF) and plane-wave local-density approximation (LDA) calculations, which give the values of 10.8[20] and 2.37 eV,[28] respectively. It is well known that the HF method tends to overestimate and LDA approach tends to underestimate the value of the gap[29] while hybrid density functionals, such as B3LYP used in this work, have been found to give reasonable band gap values.[29] Another estimate of TATB band gap was obtained by combining the results of spectroscopic measurements of TATB thin films[30] with earlier calculations of *isolated* molecules. The obtained value of 6.6 eV may have neglected the reduction of the crystalline band gap, as compared to the molecular HOMO−LUMO gap, due to the intermolecular interactions. The top of the valence band of TATB crystal is formed by the carbon and oxygen states, whereas the bottom of the conduction band is determined by the nitro-groups, which is in agreement with previous periodic LDA plain-wave calculations.[28]

Our ECM calculations suggest that the activation energy for the intramolecular hydrogen transfer in solid TATB is 76.1 kcal/mol and the reaction energy is 49.7 kcal/mol. The latter is slightly higher than that in the gas phase (36.0 and 47.5 kcal/mol for 6-31+G** and 6-21G basis sets, respectively) due to the crystalline field effect. The transfer pathway involves the rotation of the neighboring amino- and nitro- groups so as the H atom occupies a midpoint position between the N and O atoms of these groups (Figure 2a). After the bond switching, the H relaxes out of the molecular plane and finds a local energy minimum at the site between the two oxygen atoms of the nitro-group. In this final configuration, the torsion angles of the donor amino- group $\angle H-N-C_2-C_1$ and that of the hydrogen bearing nitro- group $\angle O-O-N-C_1$ are changed by 9.4° and by −3.9° relative to the initial geometry, respectively. The configuration of the benzene ring of the perturbed molecule as well as the positions of close neighbors do not change much. This is in sharp contrast with the isolated molecule calculations, where hydrogen causes a large distortion of the benzene ring and the $\angle O-O-N-C_1$ torsion angle in the hydrogen bearing nitro-group changes by −26.9°. Thus, the crystalline environment strongly affects the structure of the perturbed TATB molecule by stabilizing its benzene ring due to $\pi-\pi$ stacking and the effect of the perturbation is released through the rotation of the hydrogen bearing nitro- group.

The analysis of the charge density distribution of several molecular configurations along the H transfer path suggests that

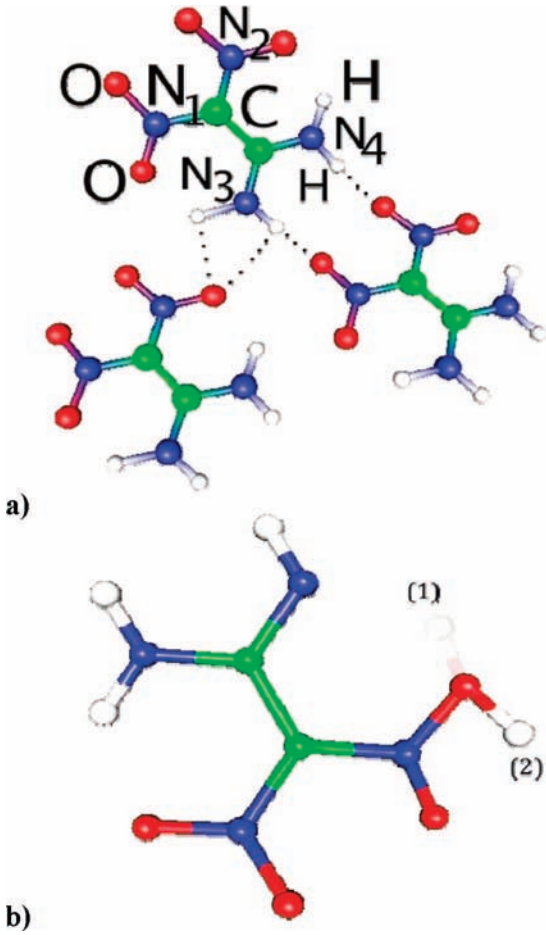

Figure 3. Arrangement of DADNE molecules in a crystalline layer. (a) DADNE with two nonequivalent connections of nitro- and amino-groups, where intermolecular hydrogen transfer may occur via pathways pointed by broken lines. (b) Possible molecular structures of the HONO-rearranged DADNE molecule.

the hydrogen migrates as a proton. The extra electron charge associated with the broken N−H bond redistributes mainly over N atoms of other amino- groups ($\Delta Q \sim 0.1$ e) and O atom forming O−H bond ($\Delta Q \sim 0.2$ e); this is accompanied by a charge density redistribution in the benzene ring.

We also note that the obtained activation energy for the hydrogen transfer in crystalline TATB (76.1 kcal/mol) is slightly higher then the upper limit of the experimental energy range (61–68 kcal/mol) for overall thermal decomposition of TATB and related nitro-compounds,[1,2] which suggests that the initiation mechanism may be more complex than a simple hydrogen migration and possibly involves the barrier reduction due to defects or cooperative phenomena.[26,27,31]

Unexpectedly, our ECM calculations demonstrate that the hydrogen migration between two neighboring molecules does not take place, in contrast with molecular calculations.[8] By systematically trying a range of different configurations for the hydrogen transfer, we could not find any local energy minimum: the hydrogen atom always relaxed back to its equilibrium position and reformed the N−H bond. We therefore conclude that the molecular model in this case leads to erroneous conclusions regarding the hydrogen transfer.

To explore the mechanisms of the inter- (Figure 3a) and intramolecular (Figure 3b) hydrogen transfer in the crystalline DADNE, we also applied the ECM described above. The shape of the QM cluster (Figure 1b) is different from that used for TATB due to the differences in the lattice structure of these materials and the dipole moment of DADNE molecules. In these calculations, we carried out the geometry optimization of the entire region I, including the QM cluster and 292 classical molecules. The electronic structure calculations yield the band gap value of 3.44 eV, which agrees well with 3.4 eV obtained from the HF calculations corrected by the many body perturbation theory for electronic correlations.[15] In the absence of experimental data, this value can be also compared with the band gap of 2.2 eV obtained in earlier periodic model DFT calculations using the PW91 exchange-correlation functional and plane-wave basis set.[26,31] The latter value is expected to be underestimated due to the known deficiencies of the PW91 density functional.[29]

In ECM calculations of the intramolecular hydrogen transfer in DADNE, we have explored as initial guesses several symmetrically nonequivalent points belonging to 3D surface, which are equidistant from oxygen atoms. We found that neither intra- nor intermolecular hydrogen transfer takes place in the solid DADNE. Indeed, regardless of the initial guess, the H atom relaxes back to the ground state geometry and does not favor binding of migrated hydrogen to oxygen atoms of the nitro- group in the same molecule or a nearest neighbor molecule (Figure 2b).[32] This conclusion implies that NO appears among the DADNE decomposition products[3,12] due to nitro-to-nitrite isomerization[10,11] and H_2O is, most likely, a result of secondary reactions.

According to the NPA analysis, hydrogen is in a positive charge state in all the configurations on the transfer path. This is similar to the case of TATB, where hydrogen is transferred in a form of a proton. However, the redistribution of the electron density due to the broken N−H bond is different in DADNE. The electron density remains mostly localized at the host nitrogen atom (its atomic charge changes from −0.7 to −0.9 *e*), while only a small amount of it is delocalized over oxygen atoms. The strong electrostatic interaction between the H^+ and the host N^- hampers the hydrogen transfer. Quite differently, in TATB, the electron density is redistributed over several symmetrically arranged N atoms. This makes the electrostatic interaction between H^+ and the host N^- ion relatively weak, so as the intramolecular transfer can take place. At the same time, the interaction of H^+ and the negatively charged molecule as a whole remains strong and, consequently, the intermolecular hydrogen transfer is unfavorable.

Conclusions

To summarize, our ECM modeling of the hydrogen transfer in DADNE and TATB demonstrates that the molecular and crystalline structures of the materials strongly affect the mechanisms of the hydrogen migration. Generally, a formation of the HONO isomers is considered to be a potential precursor for the decomposition reaction in nitro-containing explosives, and, at least in TATB, it can also mediate the formation of benzofurozan and benzofuroxan derivatives, which presumably suppresses the decomposition chemistry. Our results demonstrate that even though DADNE has similar to TATB a set of functional groups, the initiation decomposition reactions there proceed via a different mechanism as the molecular and crystalline structure of DADNE disfavors the hydrogen migration and formation of a HONO isomer unlike in TATB, where such an isomer is readily formed. We note that the results of our calculations are in contrast with earlier reports, where TATB has been represented using a molecular model. This disagreement reveals the importance of the proper account of the

intermolecular interactions and crystalline electrostatic potential in modeling reactions in the solid phase of these molecular materials.

Acknowledgment. This work is supported in part by the USA ARO MURI Grant No. W9011NF-05-1-0266. P.V.S. is supported by the Grant-in-Aid for Creative Scientific Research No. 16GS0205 from the Japanese Ministry of Education, Culture, Sports, Science and Technology. The calculations were carried out using UCL CRAG facilities. The authors are grateful to B. Rice for providing initial force-field parameters. M.M.K. is grateful to the Division of Materials Research of NSF for support under the Independent Research and Development Program. Any appearance of findings, conclusions, or recommendations expressed in this material are those of the authors and do not necessarily reflect views of the National Science Foundation.

References and Notes

(1) Brill, T. B.; James, K. J. *Chem. Rev.* **1993**, *93*, 2667.

(2) Brill, T. B.; James, K. J. *J. Phys. Chem.* **1993**, *97*, 8752.

(3) Östmark, H.; Langlet, A.; Bergman, H.; Wellmar, U.; Bemm, U. *Proceedings of the 11th International Detonation Symposium (ONR 2000)*, Snowmass, Colorado, 1998; Paper No. 33300-5, p 807.

(4) Bemm, U.; Östmark, H *Acta Crystalogr.* **1997**, *C54*, 1999.

(5) Sharma, J.; Forbes, J. W.; Coffey, C. S.; Liddiard, T. P. *J. Phys. Chem.* **1987**, *91*, 5139.

(6) Behrens, R.; Bulusu, S. In *Challenges in Propellants & Combustions 100 years after Nobel*; Kuo, K., Ed.; Begell House, Inc., 1997; pp 275–289.

(7) Land, T. A.; Siekhaus, W. J.; Foltz, M. F.; Behrens, R. *Proceedings of the 10th International Detonation Symposium (ONR 1995)*, Boston, MA, 1993; Paper No. 33395-12, p 181.

(8) Wu, C.; Fried, L. *J. Phys. Chem. A* **2000**, *104*, 4337.

(9) Politzer, P.; Concha, M. C.; Grice, M. E.; Murray, M. E.; Lane, P.; Habibollazadeh, D. *J. Mol. Struct.: THEOCHEM* **1998**, *75*, 425.

(10) Gindulyté, A.; Masaa, L.; Huang, L.; Karle, J. *J. Phys. Chem. A* **1999**, *104*, 11040.

(11) Kimmel, A. V.; Sushko, P. V.; Shluger, A. L.; Kuklja, M. M. *J. Chem. Phys.* **2007**, *126*, 234711.

(12) Gao, H.-X.; Zhao, F.-Q.; Hu, R.-Z.; Pan, Q.; Wang, B.-Z.; Yang, X.-W.; Gao, Y.; Gao, S.-L. *Chin. J. Chem.* **2006**, *24*, 117.

(13) Sushko, P. V.; Shluger, A. L.; Catlow, C. R. A. *Surf. Sci.* **2000**, *450*, 153.

(14) Sulimov, V. B.; Sushko, P. V.; Edwards, A. H.; Shluger, A. L.; Stoneham, A. M. *Phys. Rev. B* **2002**, *66*, 024108.

(15) Kuklja, M. M.; Zerilli, F. J.; Sushko, P. V. *MRS Proceedings, 800, Synthesis, Characterization and Properties of Energetic/Reactive Nanomaterials*; Armstrong, R. W., Thadhani, N. N., Wilson, W. H., Gilman, J. J., Munir, Z., Simpson, R. L., Eds.; 2004; 211–222.

(16) Kimmel, A. V.; Sushko, P. V.; Shluger, A. L.; Kuklja, M. M., in press.

(17) Frisch, J.; et al. *GAUSSIAN03*; revision C.02, Gaussian, Inc.: Wallingford CT, 2004.

(18) Becke, D. *J. Chem. Phys* **1993**, *98*, 5548.

(19) Lee, C.; Yang, W.; Parr, R. *Phys. Rev. B* **1988**, *37*, 785.

(20) Kunz, B. *Phys. Rev. B* **1996**, *53*, 9733.

(21) Spackman, M. A.; Mitchell, A. S. *Phys. Chem. Chem. Phys.* **2001**, *3*, 1518.

(22) Rice, B., private communication.

(23) Sorescu, C.; Boatz, J. A.; Tompson, D. *J. Phys. Chem. A* **2001**, *105*, 5010.

(24) Reed, A. E.; Weinstok, R. B.; Weinhold, F. *J. Chem. Phys.* **1985**, *83*, 735.

(25) Cady, H. H.; Larson, A. C. *Acta Crystalogr.* **1965**, *18*, 485.

(26) Kuklja, M. M.; Rashkeev, S. N.; Zerilli, F. *Appl. Phys. Lett.* **2003**, *82*, 1371.

(27) Kuklja, M. M.; Rashkeev, S. N. *Appl. Phys. Lett.* **2007**, *90*, 151913.

(28) Wu, C. J.; Yang, L. H.; Fried, L. E.; Quenneville, J.; Martinez, T. J. *Phys. Rev. B* **2003**, *67*, 235101.

(29) (a) Corà, F.; Alfredsson, M.; Mallia, G.; Middlemiss, D. S.; Mackrodt, W. C.; Dovesi, R.; Orlando, R. *Struct. Bond.* **2004**, *113*, 171. (b) Muscat, J.; Wander, A.; Harrison, N. M. *Chem. Phys. Lett.* **2001**, *342*, 397.

(30) Kakar, S.; Nelson, A. J.; Treusch, R.; Heske, C.; van Buuren, T.; Jimenez, I.; Pagoria, I.; Terminello, L. J. *Phys. Rev. B* **2000**, *62*, 15666.

(31) Kuklja, M. M.; Rashkeev, S. N. *Phys. Rev. B* **2007**, *75*, 104111.

(32) In ECM calculations, although a metastable configuration of HONO was eventually found in a crystalline DADNE (configuration 2 in Figure 3b), the corresponding high reaction energy (~2 eV), the high barrier (~4 eV), and the pathway profile indicate that the HONO state arises from the hydrogen diffusion or other high energy process rather than from hydrogen bond switching with nearest neighbors as it happens in TATB. This leads us to believe that the HONO formation is not a feasible candidate for the thermal initiation in DADNE, in contrast to TATB.

JP800930D